Quantitative-Structure-Property-Relationships for Longitudinal, Transverse and Molecular Static Polarizabilities in Polyynes

C.D. Zeinalipour-Yazdi* and D.P. Pullman

Department of Chemistry and Biochemistry San Diego State University, San Diego, CA 92182-1030

Abstract

In this work we present an accurate Quantitative Structure-Property Relationship (QSPR), derived from *ab initio* coupled-cluster calculations, which estimates the static molecular polarizability and bandgap in polyynes, as a function of their length. Static Molecular polarizabilities and bandgaps are computed at the CCSD(T)/cc-pVTZ//CCSD(T)/cc-pVTZ level of theory for the homologous sequence of linear polyynes, $C_{2n}H_2$ ($n \leq 9$), and compared to results for several one-dimensional quantum-mechanical model systems. In the case of independent electron models, regardless of the form of the potential, the polarizabilities increase strongly with system size, scaling as L^4, where L is the length of the model system. In contrast, the polyyne polarizabilities scale as $L^{1.64}$, where L is taken as the distance between terminal carbon atoms. The reduction in exponent is shown to arise predominantly from electron-electron repulsion in contrast to electron correlation that were found to only play a minor role. To gain deeper insight into the length dependence of the polarizability, we also analyze the distortion of the molecular orbitals in polyynes, due to the presence of an external electric field and find that occupied states at the Fermi level in large molecular weight polyynes exhibit increasingly larger distortions (polarization) in the presence of an external electric field than the corresponding states in smaller polyynes, indicative of their higher electron mobility. The extrapolated to infinite length bond

* Current address: University of Cyprus, Department of Chemistry, 75 Kallipoleos St., P.O.Box 20537, 1678 Nicosia, Cyprus. Fax: +357-22-331995. E-mail address: zeinalip@ucy.ac.cy

length alternation in linear polyynes are found to be 0.1276 Å and 0.1523 Å at the center and the termination of the chain, respectively. A comparison of the polarizabilities computed by various computational methodologies, such as Hartree-Fock, density functional theory, Møller-Plesset perturbation theory, and coupled cluster theory showed that the computationally less intensive Hartree-Fock methodology yields polarizabilities close to the coupled-cluster results, whereas conventional density functional theory methodologies overestimate the polarizabilities by as much as 60% in some occasions.

I. Introduction

A fundamental understanding of the molecular polarizability at a molecular orbital level can aid in the design and analysis of molecular systems that are held together by weak forces such as π-π interactions. Molecular polarizabilities determine the strength of interaction between non-polar molecules, as described by the London[1] equation. We have recently shown that for weak interactions, such as π-π interactions between polycyclic aromatic hydrocarbons, there is a linear correlation between the binding energy and the static molecular polarizability. [2,3] Hence, being able to compute the molecular polarizability from simplified relationships that correlate the molecular size to the molecular polarizability can prove very useful in quantifying these interactions in material coatings that are composed of polyyne-based materials. Furthermore the molecular polarizability is a physical parameter that is invoked very frequently invoked in the description of a wide range of physical phenomena, such as the interaction of photons [4] and particles with molecules[5] as well as other molecular properties such as bond dissociation energy[6], nonlinear optical properties[7] , hardness/softness[8] and electronegativity. [9] Conjugated polymers with delocalized electronic states constitute an important class of materials that exhibit non-

linear optical properties. Accurate prediction of the polarizability in long chain conjugated polymers may aid to the molecular engineering of optically active compounds with high specific linear and non-linear response in the presence of an electric field.[10] In particular, the polarizability of a material is intimately related to the refractive index[11], which is a critical parameter in the design of planar polymer waveguides[12], found in applications such as thermal optical switches[13] (TOS), variable optical attenuators[13] (VOA), optical couplers/splitters[14] and arrayed waveguide gratings[15] (AWG).

In this study, we explore the dependence of polarizability on molecular size for the series of linear polyynes, $C_{2n}H_2$, where $n \leq 9$. Polyynes are the simplest molecular system, with respect to their molecular structure, that exhibit π-conjugation. These molecules are 1-dimensional, with alternating single and triple bonds between carbon atoms, and their polarizabilities can be computed very accurately for a fairly wide range of lengths due to their high symmetry point group ($D_{\infty h}$). In particular, to minimize potential artifacts in the polarizabilities due to inadequate level of theory or basis set size, the polyyne geometries were optimized at the benchmark CCSD(T)/cc-pVTZ level (occasionally checked against aug-cc-pVTZ, cc-pVQZ, cc-pV5Z, and cc-pV6Z basis sets), and then polarizabilities were computed at the optimized geometries at several levels of theory (RHF, MP2, SCS-MP2, CCSD, CCSD(T), and DFT with B3LYP and PBE) using again the cc-pVTZ basis set (occasionally checked against aug-cc-pVTZ and cc-pVQZ basis sets).

Several authors[16] report *ab initio* computations of static polarizabilities (α_{xx}) and first hyperpolarizabilities (γ_{xxx}) of small molecular weight π-conjugated molecules, such polyenes, polyynes and comulenes. Maroulis *et al.*[17] examined polyynes $C_{2n}H_2$ ($n \leq 4$) and showed that the longitudinal static polarizability and second hyper-polarizability exhibit an $L^{1.5}$ and $L^{3.0}$ (L =

molecular length) increase, respectively. Later on Archibond *et al.*[18] using the finite field method and after studying the effects of basis set size on the computed (hyper)polarizabilities suggest $\alpha_{xx}/n = 110 \pm 10$ a.u. and $\gamma_{xxx}/n = (1.0 \pm 0.3)\times 10^{-3}$ a.u. as the infinite chain limit for the longitudinal static polarizability and first hyperpolarizability in polyynes, respectively. Other studies have focused on the effect of the π-bonding sequence[19] in the linear π-conjugated molecules on the (hyper)polarizability or even the effect of electron donating-withdrawing functional groups[20] terminating the linear chains. Champagne *et al.*[21] showed that DFT based exchange functionals, such the Becke and the Slater, overestimate significantly the static polarizability. The same authors were able to assess the Young modulus, the force constants, the vibrational frequencies, and the phonon dispersion curves for linear polyynes. [22] Other research efforts focused on methodologies that can be applied to infinite periodic systems[23,24,25] and were successfully applied to quasi-one dimensional molecule chains of water ($[H_2O]_\infty$,[26]) and molecular hydrogen[27].

In a broader context, polyynes of structure $XC_{2n}X'$ (X, X' = hydrogen and various organic and organometallic end groups) have attracted increasing interest because their significant polarizabilities, hyperpolarizabilities, and current-voltage characteristics make them potential candidates as materials in nonlinear optics and molecular electronic devices[28] and also because of their importance in interstellar chemistry and spectroscopy.[29] In addition, progress in developing methodologies for synthesizing polyynes has allowed a number of derivatives to be available in sufficient quantity for their study. Recent synthetic methodologies[30] allow the synthesis of long chain polyynes ($C_{2n}TIPS_2$, $n \leq 10$, TIPS = triisopropylsilyl) that appear to have some unusual optical properties that are length dependent. In particular, the authors show that no saturation of the second hyperpolarizability occurs, for $n \leq 10$ and that the power dependence of γ

($L^{4.28}$) is much greater than that of polyenes or polyenynes. Furthermore, the end groups have a significant effect on the physical properties of polyynes since their electron-donating or electron-withdrawing character can affect the polarizability and higher hyperpolarizability of the π-framework. [31] Electron correlation and careful choice of molecular geometry can lead to significant variations in the predicted hyperpolarizabilities of p-nitroaniline[32], polyacetylenes (PA) and polyynes.[33] Furthermore, Dalskov *et al.*[34] have performed polarizability calculations for polyynes as larger as $C_{100}H_2$ using the uncorrelated random phase approximation (RPA) and the uncorrelated random phase approximation (SOPPA) using fixed bond lengths for the triple (1.18Å) and single (1.40Å) carbon-carbon bonds. They observe a converging trend of the static longitudinal polarizability difference ($\Delta\alpha_{zz} = \alpha^{n}_{zz} - \alpha^{n-1}_{zz}$) for $n \geq 9$.

In the present study, the dependence of polarizability on system size is first determined for four model 1-dimensional systems: an electron-in-a-box, an electron undergoing harmonic motion, an electron-in-a-box with a sinusoidal potential intended to mimic the potential an electron experiences in a polyyne, and π electrons within the Hückel model. The polarizabilities of the polyynes C_2H_2 to $C_{18}H_2$ are then computed by accurate *ab initio* methods. Since the size dependence of the polyyne polarizabilities differs significantly from that of the four simplistic models, we seek for an explanation of this phenomenon by systematically studying the polarizabilities of H_2^+ and H_2 as a function of internuclear distance and by analyzing the distortion of individual molecular orbitals, in C_8H_2 and the particle-in-box, due to the presence of a uniform external electric field.

II. Computational Methods

The finite–field method[35] was used to compute the polarizability parallel (longitudinal) and perpendicular (transverse) to the molecular axis of the polyynes and of H_2^+ and H_2. In this method, a molecule's energy is computed at a series of applied electric fields, and the static polarizability and hyperpolarizabilities are then determined from the derivatives at zero field of the energy with respect to electric field. If the electric field $\varepsilon_{//}$ is applied along the molecular axis, then a Taylor series expansion of the energy E about $\varepsilon_{//}=0$ gives,

$$\begin{aligned} E &= E^{(0)} + \left(\frac{dE}{d\varepsilon_{//}}\right)_0 \varepsilon_{//} + \frac{1}{2}\left(\frac{d^2E}{d\varepsilon_{//}^{\,2}}\right)_0 \varepsilon_{//}^{\,2} + \frac{1}{6}\left(\frac{d^3E}{d\varepsilon_{//}^{\,3}}\right)_0 \varepsilon_{//}^{\,3} + \frac{1}{24}\left(\frac{d^4E}{d\varepsilon_{//}^{\,4}}\right)_0 \varepsilon_{//}^{\,4} + \cdots \\ &= E^{(0)} - \mu_{//}\,\varepsilon_{//} - \frac{1}{2}\alpha_{//}\,\varepsilon_{//}^{\,2} - \frac{1}{6}\beta_{//}\,\varepsilon_{//}^{\,3} - \frac{1}{24}\gamma_{//}\,\varepsilon_{//}^{\,4} + \cdots \end{aligned} \quad (1).$$

Thus, the static longitudinal and transverse polarizability are defined as,

$$\alpha_{//} = -\left(\frac{d^2E}{d\varepsilon_{//}^{\,2}}\right)_0 \text{ (2), and } \alpha_{\perp} = -\left(\frac{d^2E}{d\varepsilon_{\perp}^{\,2}}\right)_0 \text{ (3), respectively.}$$

Note that for centro-symmetric molecules such as the polyynes ($C_{2n}H_2$), odd order terms in the energy expansions are zero by symmetry. Thus only even ordered terms are evaluated in order to obtain the longitudinal and transverse polarizability.

The molecular polarizability is very sensitive to molecular geometry, and in particular on the degree of bond length alternation, thus all polyynes were first optimized at a very high level of theory, CCSD(T), and with a relatively large basis set, Dunning's correlation-consistent polarized valence triple-zeta (cc-pVTZ) basis set. [36] Optimization was performed using the numerical optimization capability of the software package, Molpro 2006.1. [37] The default of allowing valence, but not core, electron correlation was used. Convergence of the bond lengths with respect to basis set was tested for the smaller molecular weight (MW) polyynes (C_2H_2,

C_4H_2, C_6H_2, and C_8H_2), using larger basis sets, such as the cc-pVQZ and aug-cc-pVTZ. The effect of an applied electric field (0.004 au, highest field strength used) on the equilibrium structure geometries was also briefly investigated for the smaller MW polyynes, at the CCSD(T)/cc-pVTZ level of theory. No evidence of molecular distortion at this electric field strength could be observed.

Polarizabilities at the CCSD(T)/cc-pVTZ optimized geometries were then computed for C_2H_2 through $C_{18}H_2$ using a range of theory levels, including RHF, MP2, SCS-MP2 (Ref. [38]), CCSD, and CCSD(T) as well as DFT with the B3LYP and PBE exchange-correlation functionals. The cc-pVTZ basis set was used, and results for several molecules were checked against those of two larger basis sets, the aug-cc-pVTZ and cc-pVQZ. The electric fields strengths used in the finite-field computations were 0, 0.002, and 0.004 au (1 au = 5.14 x 10^{11} V/m). To ensure that higher order terms in Eq. (1) are unimportant at these electric field strengths, a number of polarizability computations were also performed at fields one order of magnitude smaller, i.e., 0, 0.0002, and 0.0004 au to ensure agreement with the results obtained at larger electric fields.

For the particle-in-a-box (PIB) system in which the potential energy varied sinusoidally inside the box, energies and wavefunctions were determined numerically as a function of electric field by solving the Schrödinger equation with the shooting method. [39] A dedicated program written in Maple 9 was developed for this purpose. [40]

III. Results and Discussion

The presentation of our results will be given in the following order. First we present the polarizability trends as a function of length (L) of various simple quantum mechanical systems

that lack electron-electron repulsion, such as the one-dimensional particle-in-box (1D-PIB), the one-dimensional simple harmonic oscillator (1D-SHO), the 1D-PIB under the influence of a sinusoidal potential and the polarizability of the molecular hydrogen cation (H_2^+). Then we compare to the polarizability trends of the homologous molecular sequence of linear polyynes $C_{2n}H_2$ ($n \leq 9$) and discuss the trends observed.

A. Simplified quantum mechanical model systems

1) Analytic polarizability for 1D-PIB: The Schrödinger equation for a particle in a 1-dimensional box (1D-PIB) subjected to a uniform electric field ε can be solved either exactly, with the wavefunctions expressed in terms of Airy functions,[41,42] or more simply via perturbation theory. [41,43] In either case, the polarizability is given by Eq. (3). If the particle is an electron and the potential energy operator is $\hat{V} = \hat{\mu}_x \cdot \hat{\varepsilon} = -e \cdot \varepsilon \cdot x$, the polarizability of the electron in state n is derived in Appendix A and given by,

$$\alpha_{xx} = \frac{64e^2 m_e n^2 L^4}{\pi^6 \hbar^2} \sum_{k \neq n} \frac{k^2 \left[(-1)^{n+k} - 1\right]^2}{\left(k^2 - n^2\right)^5} \qquad (4).$$

Here, m_e is the electron mass, L the length of the box, ħ Planck's constant divided by 2π, e the elementary charge of an electron, and n and k the quantum numbers of the n^{th} and k^{th} energy states, respectively. As shown in Eq. (4), the polarizability scales as the fourth power of the length for any state n. The interesting feature of the 1D-PIB and polyyne polarizability calculations is that comparison of their wavefunctions show great similarity, nonetheless their polarizability length dependence scales very differently, L^4 and $L^{1.64}$, respectively, as shown in subsequent section.

2. *Analytic polarizability of 1D-SHO:* The Schrödinger equation for an electron bound harmonically to a positive charge and subjected to an electric field has an analytical solution. [43]

The result is that the energy of all harmonic oscillator states are shifted down by $e^2\varepsilon^2$ / (2k), where k is the force constant. Thus, the polarizability is $\alpha = e^2$ / k, which of course is always positive, in contrast to all other systems studied here. To express the polarizability in terms of an extent of motion, we take the "length" L of the oscillator as twice the classical turning point, x_{tp}. One can show that,

$$\alpha = \frac{m_e e^2 L^4}{\hbar^2 (v + \frac{1}{2})^2} \qquad (5)$$

,where m_e is the mass of the electron, and ν is the quantum number. Thus, as in the particle-in-a-box case, the polarizability scales with the fourth power of distance.

3. Numerical polarizability of 1D-PIB with sinusoidal potential: The third model system considered is a modified PIB in which the potential inside the box varies sinusoidally with position. This modification was made to approximately mimic the coulombic potential an electron experiences due to the nuclei in polyynes. The potential inside the box is given by,

$$\hat{V} = \mathrm{A} \cdot \sin\left[\frac{2\pi}{\lambda}(\mathrm{x} + \varphi)\right] - e \cdot \varepsilon \cdot \mathrm{x} \qquad (6)$$

, where A, λ, and φ are the amplitude, period, and phase of the potential, respectively. Since the Schrödinger equation with such a potential does not have an analytical solution, wavefunctions and energies were determined numerically via the shooting method[39] (see Appendix A) using a devoted computer program written in Maple.[40]

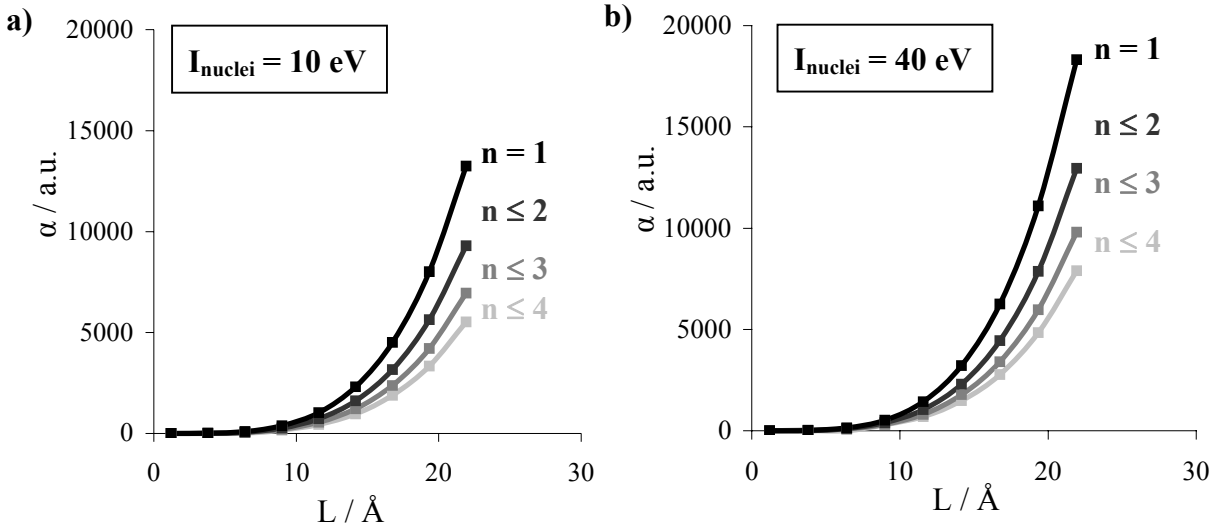

FIG. 1. Static longitudinal numerical polarizabilities 1D-PIB with sinusoidal potential amplitudes of 10 and 40 eV as a function of box length (L).

In order to examine the effect of the nuclei potential onto polarizability of the 1D-PIB we evaluated the polarizability systems that contained up to 4 electrons (n = 4). In Fig.1 we show the static longitudinal numerical polarizabilities 1D-PIB with sinusoidal potential amplitudes of 10 and 40 eV as a function of box length (L). The results here clearly indicate that introduction of the sinusoidal potential generally increases the polarizability of a quantum system. This suggests. For a nuclei amplitude of 10 eV, the increase is typically 2-3% compared to the value obtained using a zero amplitude sinusoidal potential, while for an amplitude of 40 eV, the increase is as large as 40% in some cases. From these results we expect that for polyynes the increase in polarizability due to the potential of the nuclei will be 2-3%, since the actual nuclei potential the electrons feel in conjugated π-systems based on the ionization potential[44] (IP) of ethylene (12.2eV) and acetylene (12.3eV) is of the order of 10 eV. Fitting of a power function of the form $y = \mathbf{a}\cdot x^{\mathbf{b}}$ yielded **b** = 4 for all curves and an **a** that roughly linearly decreases with the number of electrons in the system (n). The scaling of the polarizability with system size is essentially L^4, for a given states and sinusoidal amplitude similar to the 1D-PIB and the 1D-SHO.

4. Polarizability of H_2^+ and H_2: The molecular hydrogen cation (H_2^+) is one of the few molecular systems where electron-electron repulsions are absent. Thus, the Hartree-Fock method is sufficient to yield accurate results and basis set saturation is relatively computationally inexpensive. The one electron wavefunction of H_2^+ were expanded within the aug-cc-pVQZ basis with the use 114 primitive gaussians to ensure near basis set saturation. We evaluated the second derivative of the energy with respect to the electric field to obtain the longitudinal and transverse polarizabilities, α_{xx} and α_{zz}, respectively (Fig. 2).

The static polarizability of the molecular hydrogen cation scales as $L^{3.9}$, in very close agreement with the L^4 dependence of the simple quantum mechanical systems that lack electron-electron repulsion (1D-PIB, 1D-SHO). The small difference between the two can be attributed to the potential well in H_2^+, is not infinitely steep at the boundaries of the quantum mechanical system. It is evident that the L^4 scaling of the polarizability applies also to simple three-dimensional molecular systems in which electron-electron repulsion is absent. Another interesting feature in the static polarizability of H_2^+ and H_2 is that the polarizability (α_{zz}) vertical to the internuclear axis is roughly constant and scales linearly with the inter-nuclear hydrogen separation ($L^{1.164}$ and $L^{1.056}$, respectively). This is expected since the "box" length in the z direction (and y direction) is roughly constant with respect to variation of the hydrogen-hydrogen bond length. Concerning the polarizability along the molecular axis the reduction of the polarizability length dependence, from $L^{3.916}$ to $L^{2.056}$ can be attributed to the existence of *electron-electron repulsion* that is absent in the H_2^+ and present in H_2. We will see in the subsequent section that the increase of electron-electron repulsion causes the coefficient of L to further decrease, reducing further the nonlinear polarizability characteristics of the molecule.

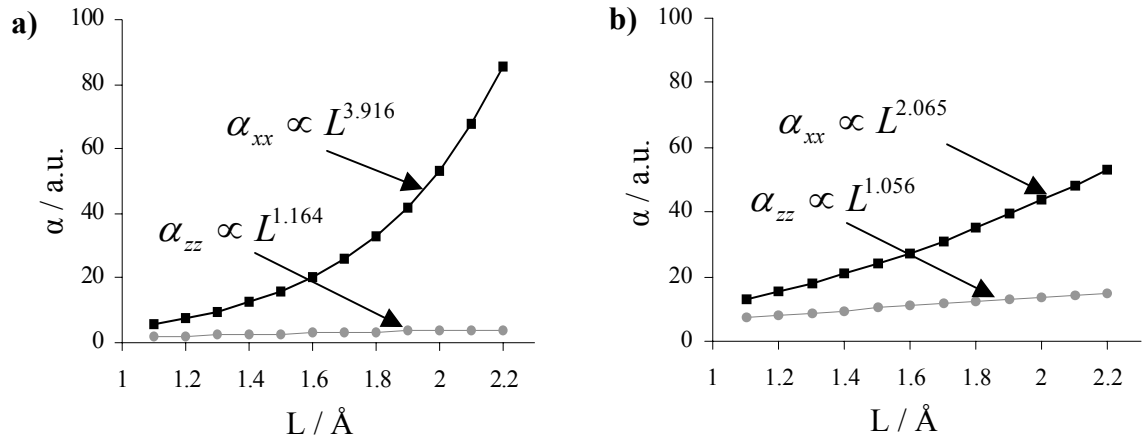

FIG. 2. Static polarizability of molecular hydrogen cation (H_2^+) and molecular hydrogen (H_2) as a function of the internuclear hydrogen-hydrogen distance (L). Calculation carried out at UHF/aug-cc-pVQZ level theory.

TABLE I. Restricted Hartree-Fock (RHF) optimized molecular geometries of $C_{10}H_2$ using various basis sets. All values are given in Angstroms.

Labels[a]	ccpVDZ	augccpVDZ	ccpVTZ	augccpVTZ	augccpVQZ
r(H-C_1)	1.064	1.062	1.054	1.054	1.054
r(C_1≡C_2)	1.194	1.194	1.183	1.183	1.182
r(C_2-C_3)	1.386	1.385	1.379	1.379	1.380
r(C_3≡C_4)	1.198	1.197	1.186	1.186	1.186
r(C_4-C_5)	1.381	1.380	1.374	1.375	1.375
r(C_5≡C_6)	1.199	1.198	1.187	1.187	1.187

[a] Numbering scheme of the carbon atoms in $C_{10}H_2$:
H—C_1≡C_2—C_3≡C_4—C_5≡C_6—C_7≡C_8— C_9≡C_{10}— H

B. Polyynes

1. Optimized molecular geometries Previous workers have found that computed polarizabilities of polyynes are sensitive to the single and triple carbon-carbon bond lengths used.[45] Consequently, in this study we have examined a series of basis sets for 1,3,5,7,9-decapentayne ($C_{10}H_2$) to determine the one that would result in convergence of the geometric parameters of $C_{10}H_2$ to within a thousand of an Angstrom. These results are tabulated in Table I and show that

the cc-pVTZ basis set is sufficient to yield molecular geometries of aug-cc-pVQZ quality. Additionally, we briefly investigated the possible influence of core-valence correlation on the optimized geometries of C_4H_2 and C_6H_2, using Dunning's correlation-consistent polarized core-valence triple-zeta basis set[36] (cc-pcVTZ) and allowing all core orbitals to participate in the electron correlation computation. We observe that bond length differences due to inclusion of core orbitals in the optimizations are less than 0.0005 Å compared to cc-pVTZ optimizations, thus the computationally less expensive cc-pVTZ basis set was eventually used. Table II presents the CCSD(T)/cc-pVTZ optimized geometries for C_2H_2 through $C_{18}H_2$ The bond length alternation ($\Delta\delta$) in an infinite polyyne chain approaches the value of 0.1276Å whereas $\Delta\delta$ close to the polyyne terminals is 0.1523 Å. Recently the bond length alternation of polyynes has been estimated to be 0.13Å in very good agreement with our present findings. [46] This range of bond length alterations is due to the edge effect caused by the finite size of these polyynes. The extrapolated single and triple carbon-carbon bond lengths in polymeric polyynes are 1.357 Å and 1.229 Å, respectively. Comparison of the CCSD(T)/cc-pVTZ optimized bond lengths to the existing gas phase experimental bond length data[47,48] of acetylene (C_2H_2) and 1,3-butadiyne (C_4H_2) shows excellent agreement.

TABLE II. Optimized CCSD(T)/cc-pVTZ bondlengths, distance L between terminal carbon atoms, and bond length alternation for the carbon atoms in the middle (Δr_{mid}) and at the ends (Δr_{end}) of the polyynes. All distances are in Angstroms. Values of Δr_{mid} and Δr_{end} extrapolated to the infinite chain are given in the final column. Values in parentheses are the corresponding experimental gas phase bondlengths taken from Ref. [47] and [48] for C_2H_2 and C_4H_2, respectively.

Labels[a]	C_2H_2	C_4H_2	C_6H_2	C_8H_2	$C_{10}H_2$	$C_{12}H_2$	$C_{14}H_2$	$C_{16}H_2$	$C_{18}H_2$	$C_\infty H_2$
r(H-C_1)	1.0637 (1.059)	1.0639 (1.062)	1.0640	1.0642	1.0643	1.0643	1.0644	1.0644	1.0644	—
r(C_1≡C_2)	1.2097 (1.209)	1.2150 (1.206)	1.2165	1.2169	1.2171	1.2171	1.2171	1.2172	1.2172	—
r(C_2-C_3)	—	1.3789 (1.380)	1.3725	1.3707	1.3701	1.3698	1.3696	1.3696	1.3696	—
r(C_3≡C_4)	—	—	1.2219	1.2240	1.2247	1.2249	1.2250	1.2251	1.2251	—
r(C_4-C_5)	—	—	—	1.3647	1.3626	1.3617	1.3613	1.3611	1.3610	—
r(C_5≡C_6)	—	—	—	—	1.2263	1.2271	1.2274	1.2276	1.2276	—
r(C_6-C_7)	—	—	—	—	—	1.3601	1.3592	1.3588	1.3586	—
r(C_7≡C_8)	—	—	—	—	—	—	1.2280	1.2283	1.2285	—
r(C_8-C_9)	—	—	—	—	—	—	—	1.3583	1.3578	—
r(C_9≡C_{10})	—	—	—	—	—	—	—	—	1.2287	—
L	1.2097	3.8089	6.3998	8.9878	11.5750	14.1614	16.7474	19.3334	21.9191	—
Δr_{mid}	—	0.1639	0.1505	0.1407	0.1363	0.1330	0.1313	0.1299	0.1291	0.1276
Δr_{end}	—	0.1639	0.1560	0.1537	0.1530	0.1526	0.1525	0.1524	0.1523	0.1523

[a] Numbering scheme of the carbon atoms in the polyyne, illustrated for C_8H_2:
H—C_1≡C_2—C_3≡C_4—C_5≡C_6—C_7≡C_8—H

2. Polarizability: All polyyne geometries in this work were optimized at the same level of theory that subsequent polarizability calculations are carried out due to the sensitivity of the polarizability on the molecular geometry adopted. [45] As we will show in section I, the optimized molecular structures exhibit a strong bond length alternating ($\Delta\delta$) character. The carbon-carbon framework alternates between triple (~1.2172 Å) and single (~1.3696 Å) carbon-carbon bonds. This phenomenon has been explained in terms of the first order Peierls[49] distortion that result in $\Delta\delta$ and the formation of a significant bandgap (HOMO-LUMO) at the Fermi level. Conjugated π-systems with a high degree of $\Delta\delta$ are considered semiconductors[50] in contrast to zero-bandgap π-conjugated molecules that have metallic properties. Previous studies have shown that the

degree of Δδ will decrease the static longitudinal polarizability that is considerably weaker than the dependence on the length of the π-conjugated chain. Fig. 3 shows the dependence of the static longitudinal and transverse polarizability as a function of the molecular length in polyynes.

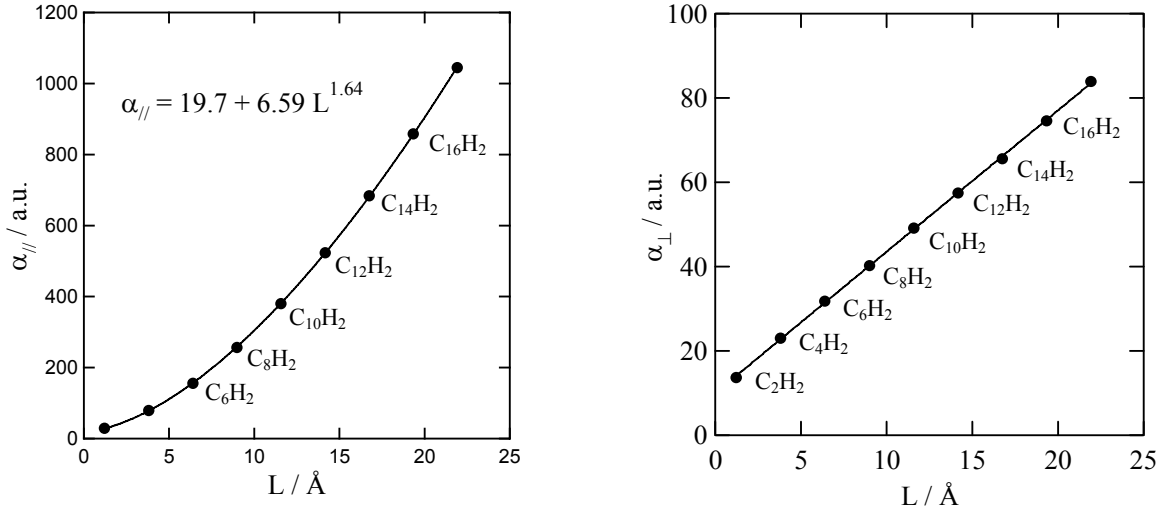

FIG. 3. Static (a) longitudinal and (b) transverse polarizability of polyynes ($C_{2n}H_2$, n≤9) as a function of molecular length (L). Calculation carried out at the CCSD(T)/cc-pVTZ // CCSD(T)/cc-pVTZ level of theory. A polarizability of 1 a.u. is equal to 1.648778 x 10^{-41} C^2m^2/J.

The graphs exhibit a linear and non-linear dependence of the longitudinal and transverse polarizability as a function of molecular length. Both curves when fit by a power function of the form $a + b \cdot L^n$ yield an exponent n of 1.64 and 1.00, respectively. A similar value (n = 1.5) for the static longitudinal polarizability is found by Maroulis *et al.*[17] in smaller MW polyynes (n ≤ 4) using smaller basis sets. Static molecular polarizabilities are not directly comparable to experimental dynamic polarizabilities obtained from Kerr effect measurements thus limited experimental measurement static polarizabilities are available in the literature. Keir *et al.*[51] report values of 5.21, 3.21, 3.88 ± 0.08 ($10^{-40} \cdot C^2m^2J^2$) for the transverse, longitudinal and molecular polarizability of acetylene (C_2H_2), respectively. We find at CCSD(T)/aug-cc-pVTZ//CCSD(T)/cc-pVTZ 5.07, 3.11, 3.76 ($10^{-40} \cdot C^2m^2J^2$), respectively. Comparison of the

experimental and theoretical values shows that this level of theory underestimates the experimental polarizabilities by only 3%. Nevertheless, due to the prohibitive basis set size of aug-cc-pVTZ for larger MW polyynes we eventually used CCSD(T)/cc-pVTZ//CCSD(T)/cc-pVTZ to study the performance of various methodologies in the assessment of polarizability compared to the higher-level coupled-cluster results. Thus molecular geometries and polarizabilities were calculated using a wide range of methodologies (e.g. RHF, MP2, SCSMP2, CCSD, B3LYP and PBE). In Table III and IV we present the static longitudinal and transverse polarizability in polyynes with the various computational methods examined. The percent difference (%diff) is a measure of the agreement between the various methods and the high-level CCSD(T) results. We observe that for the longitudinal polarizability RHF, MP2, SCSMP2 and CCSD perform well compared to CCSD(T), whereas commonly used DFT methods (B3LYP, PBE) overestimate considerably the polarizability, in some cases by 60%. This picture changes for the static transverse polarizability ($\alpha_{//}$) in polyynes where all methodologies seem to perform well to within 5-6% accuracy. This suggest that the polarizability errors that are present in DFT methods appear only along the molecular axis where error introduced by the inaccurate description of the XC functionals are stronger due to increased orbital overlap.

TABLE III. Comparison of the static longitudinal polarizability ($\alpha_{//}$) in polyynes ($C_{2n}H_2$, $n \leq 9$) computed using CCSD(T)/cc-pVTZ//CCSD(T)/cc-pVTZ to other *ab initio* and density functional theory methods. The molecular length (L) is taken as the distance between the terminal carbon atoms in the optimized molecules. The percent difference is given by, %diff = $[\alpha_{CCSD(T)} - \alpha_i] \cdot 200 / [\alpha_{CCSD(T)} + \alpha_i]$, where i = RHF, MP2, SCS-MP2, CCSD, B3LYP or PBE.

	L / Å	$\alpha_{//}$ / a.u. CCSD(T)	% diff RHF	% diff MP2	% diff SCS-MP2	% diff CCSD	% diff B3LYP	% diff PBE
C_2H_2	2.2861	29.5	4.2	-1.1	-0.9	-0.4	3.6	3.5
C_4H_2	7.1977	79.6	4.0	-0.3	-1.3	-1.7	8.9	10.7
C_6H_2	12.0939	155.7	3.2	0.6	-2.0	-3.0	14.3	18.2
C_8H_2	16.9845	256.6	2.4	1.7	-1.5	-4.3	19.4	25.7
$C_{10}H_2$	21.8736	380.0	1.5	2.8	-1.4	-5.5	24.6	33.3
$C_{12}H_2$	26.7611	523.6	0.6	3.9	-1.4	-6.6	29.6	41.0
$C_{14}H_2$	31.6481	684.0	-0.2	4.7	-1.5	-7.6	34.7	48.9
$C_{16}H_2$	36.5348	858.0	-0.9	5.5	-1.5	-8.5	39.8	57.0
$C_{18}H_2$	41.4211	1044.8	-1.7	6.2	-1.6	-9.4	44.6	65.1

TABLE IV. Comparison of the static transverse polarizability ($\alpha_{\perp}$) in polyynes ($C_{2n}H_2$, $n \leq 9$) computed using CCSD(T)/cc-pVTZ//CCSD(T)/cc-pVTZ to other *ab initio* and density functional theory methods. The molecular length (L) is taken as the distance between the terminal carbon atoms in the optimized molecules. The percent difference is given by, %diff = $[\alpha_{CCSD(T)} - \alpha_i] \cdot 200 / [\alpha_{CCSD(T)} + \alpha_i]$, where i = RHF, MP2, SCS-MP2, CCSD, B3LYPor PBE.

	L / Å	$\alpha_{\perp}$ / a.u. CCSD(T)	% diff RHF	% diff MP2	% diff SCS-MP2	% diff CCSD	% diff B3LYP	% diff PBE
C_2H_2	2.2861	13.7	3.1	-1.4	-1.4	-0.2	3.1	3.9
C_4H_2	7.1977	23.0	2.9	5.5	5.5	-1.1	2.3	2.9
C_6H_2	12.0939	31.7	4.1	1.1	-6.8	-0.1	3.3	3.6
C_8H_2	16.9845	40.2	5.5	2.3	2.3	-0.1	4.4	4.7
$C_{10}H_2$	21.8736	49.1	5.3	0.6	0.5	-0.1	4.1	4.4
$C_{12}H_2$	26.7611	57.4	6.2	2.3	1.2	-0.0	4.9	5.1
$C_{14}H_2$	31.6481	65.5	7.3	2.5	3.5	0.1	5.9	6.1
$C_{16}H_2$	36.5348	74.6	6.8	2.5	2.4	0.1	5.4	5.6
$C_{18}H_2$	41.4211	83.9	6.1	1.5	0.3	0.1	4.7	4.9

Finally we report a Quantitative-Structure-Property-Relationship (QSPR) that that can be used as a predictive tool to obtain coupled-cluster quality static longitudinal and transverse polarizabilities in polyynes as a function of their length (L). These relationships are

$$\alpha_{//} = (3.248 + 0.384\ L^{1.64}) \times 10^{-40}\ C^2m^2/J^2 \qquad (7),$$

$$\alpha_{\perp} = (1.613 + 0.302\ L^{1.00}) \times 10^{-40}\ C^2m^2/J^2 \qquad (8)$$

,where L is the length between terminal carbon atoms. was obtained by fitting a second order polynomial and a straight line to the longitudinal and transverse polarizability as a function of L, respectively, and then using the definition of the average static molecular polarizability the average static molecular polarizability which is given by

$$\alpha = (0.226L^2 + 6.526L + 11.784) \times 10^{-41}\ C^2m^2/J^2 \qquad (9).$$

3. Wavefunctions: Another very interesting feature we examine in this work is the shape of MOs in polyynes and the 1D-PIB and the effects of an electric field to them. Fig. 4 compares the wavefunctions of the 1D-PIB and the molecular orbitals found in a polyyne. The molecular orbitals shown correspond to all the valence σ- and π- orbitals in 1,3,5,7-octatetrayne (C_8H_2). In both quantum mechanical systems the energy of the molecular orbitals or wavefunctions increases as a function of the number of nodes. In particular π-orbitals are doubly degenerate having a node either along the σ_{xy} or σ_{xz} plane and are also higher in energy than the σ-band. Our computations show that the core, σ- and π- electronic bands in polyynes are completely separated. The molecules also have a considerably large bandgap that progressively decreases for higher MW polyynes. A comparison between the molecular orbitals of C_8H_2 (Fig. 4b) to the 1D-PIB (Fig. 4c) shows the good agreement of the MOs obtained from the relatively simplistic single electron PIB approach to that of a multi-electron, molecular system.

In Fig. 5 we study the influence of an electric field onto the shape of the n = 1, π- and σ-orbitals in the (a) 1D-PIB and (b,c) C_8H_2. The top images show the symmetric shape of the orbitals in the absence of an electric field. The situation changes once the electric field is turned on. There we observe a shift of the orbitals towards the positive end of the electric field. This behavior is in agreement with the common notion where the negative charge of the electronic

distribution is attracted by the positive end of the electric field. Furthermore, it can be seen that large distortions are present in the molecules of greater chain length. This result correlates well with the L^4 dependence of the longitudinal polarizability found earlier for the 1D-PIB.

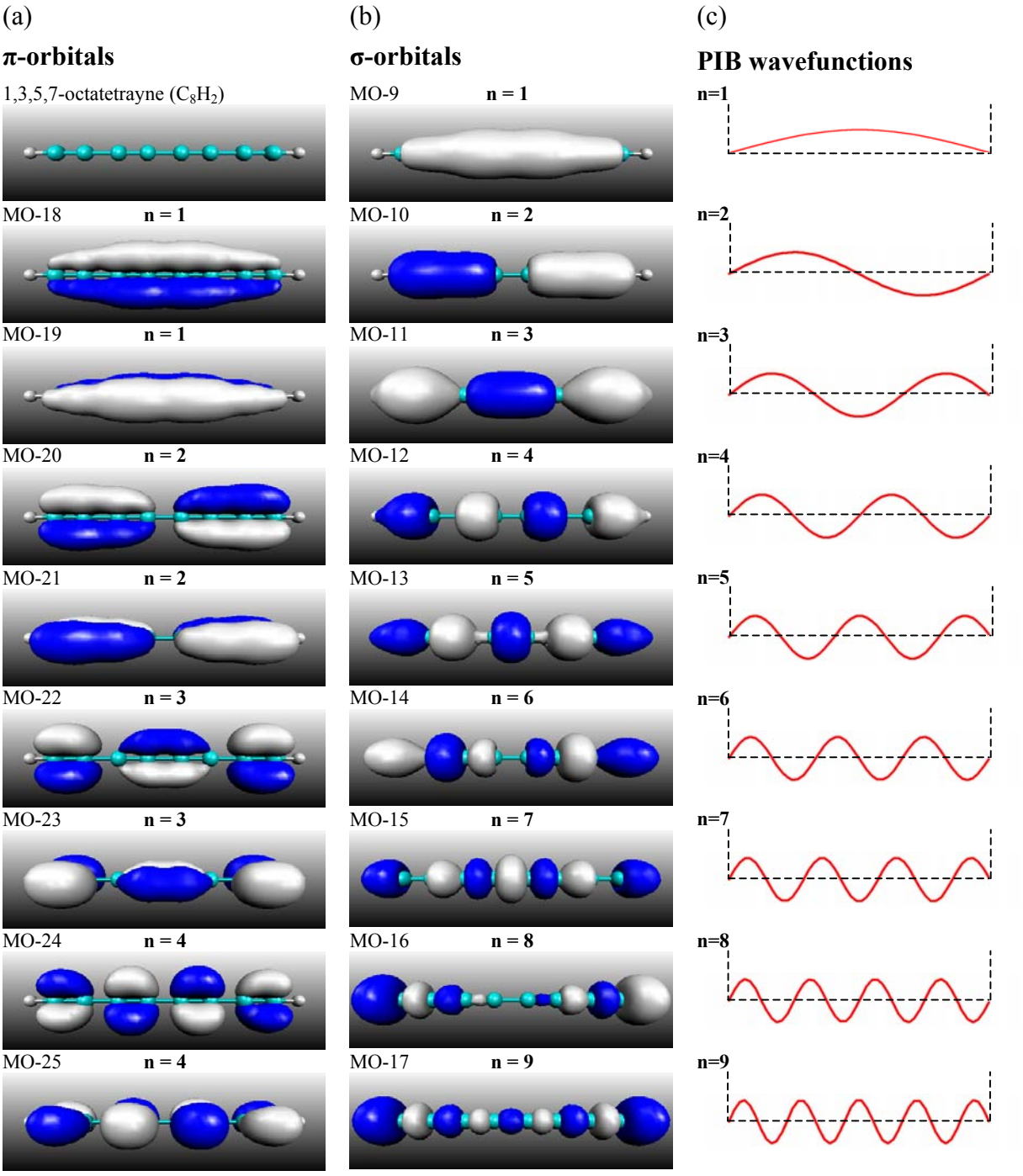

FIG. 4. Two-electron wavefunction isosurfaces of 1,3,5,7-octaterayne (C_8H_2) and 1D-PIB. (a) Three-dimensional isosurface of occupied π-orbitals and (b) σ-orbitals of C_8H_2. (c) 1D-PIB wavefunctions for n =1 through n=9.

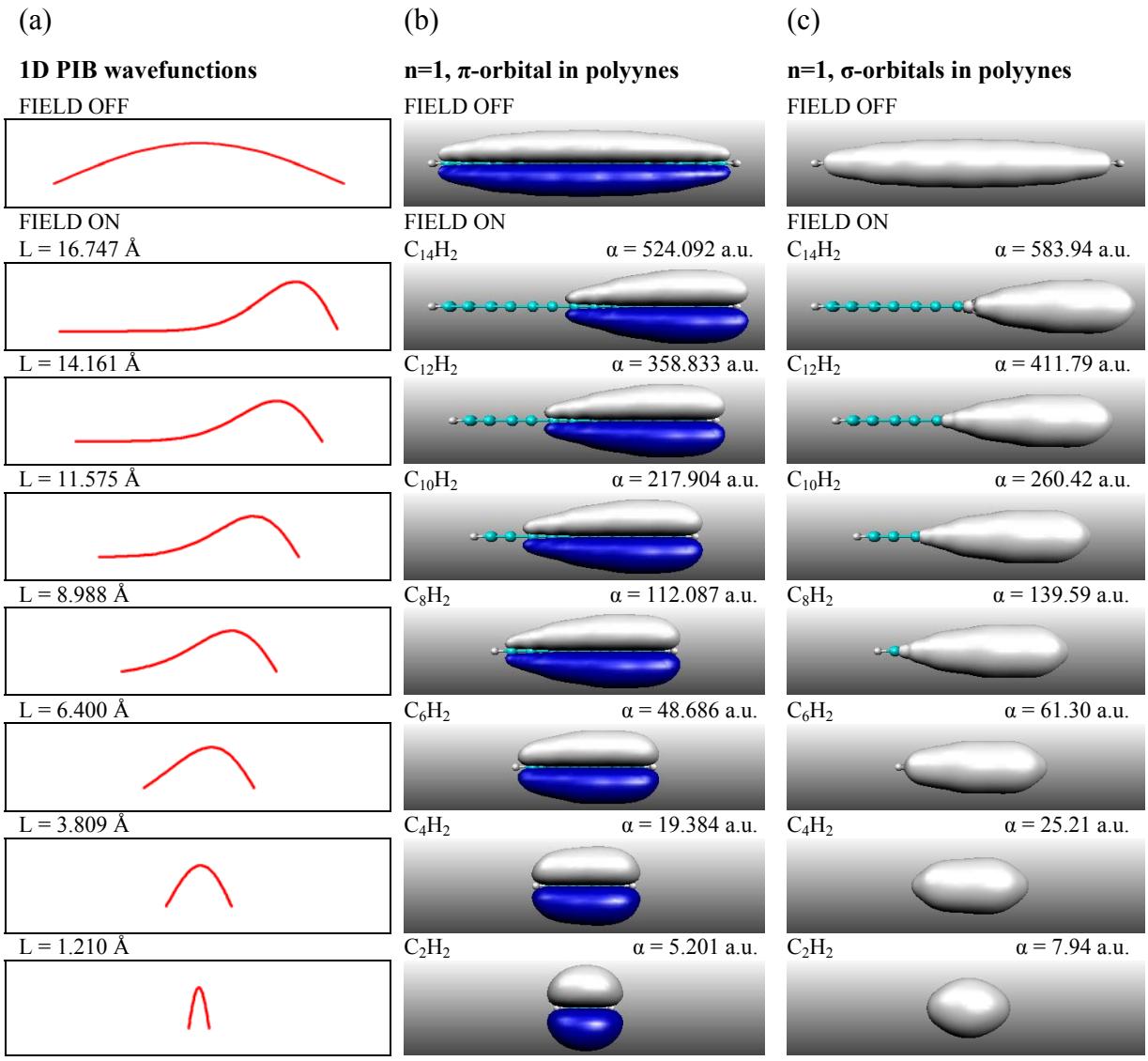

FIG. 4. Isosurface of the (a) n=1 wavefunction in the 1D-PIB, (b) π-orbitals, and (c) σ-orbitals of the homologous molecular sequence $C_{2n}H_2$. Polyyne geometries were optimized at the CCSD(T)/cc-pVTZ level of theory and polarizabilities and wavefunctions computed at the RHF/cc-pVTZ level. The electric field strength was set to 0.01 a.u. to make the polarization of the orbitals visually obvious. Isosurfaces were obtained at a cutoff value of 0.01 au. For the PIB, the length (L) is set to the terminal carbon-terminal carbon separation of the corresponding polyyne.

Conclusions

In independent electron models, such as the 1-dimensional particle-in-box in the presence and in the absence of a sinusoidal nuclei potential, the harmonic oscillator, and the molecular hydrogen cation (H_2^+) the polarizabilities scale as L^4, where L is the length of the model system.

Such a strong length dependence would be very desirable in order to enhance the nonlinear optical properties of a material. In contrast, in a multi-electron molecular system, where electron-electron repulsion is present the exponent of the polarizability length dependence is significantly smaller, reducing at the same time the nonlinear properties of a material. For polyynes the static longitudinal polarizability scales as $L^{1.64}$ whereas for molecular hydrogen it scales as $L^{2.06}$. To provide an explanation for the exponent decrease we carry out an extensive comparison of the polarizability calculated on various simple quantum mechanical systems that lack electron-electron repulsion as well as electron correlation and compare these to methods that take in account electron-electron repulsion (Hartree-Fock theory) and electron correlation (Coupled cluster theory). Our findings show that the excellent performance of the RHF method in calculating polarizabilities with respect to the computationally intensive CCSD(T) method suggests that the decrease the exponent cannot be attributed to *electron correlation effects* in contrast to first and second order hyperpolarizability computations where such effects were found to be important.[45] Furthermore comparison of the longitudinal polarizability of the molecular hydrogen cation (H_2^+), a system that inherently lacks electron-electron repulsion, and molecular hydrogen (H_2), shows that decrease of the polarizability length dependence is mainly attributed to the existence of electron-electron repulsion. We explore the effect of an isotropic electric field on the shape of the wavefunctions of the 1D-PIB and σ- and π-orbitals in polyynes and show that molecular orbitals with relatively few nodes undergo considerable polarization towards the positive end of the electric field where the non-linear ($L^{1.64}$) increase of the polarizability as a function of polyyne length suggests the possibility of higher electron mobility along the longitudinal axis, which is attributed to the conjugated π-system. At the infinite chain length limit our highly accurate CCSD(T)/cc-pVTZ optimizations showed a bond length

alternation of 0.1276 Å in the center of polyynes, which suggest that all polyynes, regardless of size remain semiconductors. Finally, we derive a Quantitative-Structure-Property-Relationship (QSPR) for the prediction of static longitudinal, transverse and molecular polarizabilities in polyynes.

Acknowledgments

We thank PURE Bioscience of El Cajon, California, for partial funding support of the computer resources.

Appendix A

Derivation of Eq. 4: Analytic polarizability for 1D-PIB

The expression of the second order correction to the energy derived from non-degenerate time-independent perturbation theory is,

$$E_n^{(2)} = \sum_{n \neq k} \frac{\left\langle \Psi^{(0)}_k \left| \hat{H}' \right| \Psi^{(0)}_n \right\rangle \left\langle \Psi^{(0)}_n \left| \hat{H}' \right| \Psi^{(0)}_k \right\rangle}{E_k^{(0)} - E_n^{(0)}} \qquad (9)$$

,where $\Psi^{(0)}_k$ and $\Psi^{(0)}_n$ are the zeroth order wavefunctions, and $E_k^{(0)}$ and $E_n^{(0)}$ the zeroth order eigenvalues of the k^{th} and n^{th} energy levels, respectively. These for the 1D-PIB confined to a potential energy well that is zero between *0* and *L (0 < x < L*), but infinite outside that range are given by Eqns. (10) and (11).

$$\Psi^{(0)}_n = \sqrt{\frac{2}{L}} \cdot sin\left(\frac{n \pi x}{L}\right), \quad (10),$$

$$E_n = \frac{n^2 h^2}{8 m_e L^2}, \quad (11), \text{ where } n = 1, 2, 3, \ldots .$$

The perturbation Hamiltonian in the *x*-direction is given by,

$$\hat{H}' = \hat{\mu}_x \cdot E = -e \cdot E \cdot x \text{ , (12).}$$

Substitution of the perturbation Hamiltonian into Eqn. 9 yields the following expression for the 2nd order corrected energy of a wavefunction,

$$\mathrm{E}_n^{(2)} = e^2 \cdot E^2 \sum_{n \neq k} \frac{\left\langle \Psi^{(0)}{}_k \left| \hat{x} \right| \Psi^{(0)}{}_n \right\rangle \left\langle \Psi^{(0)}{}_n \left| \hat{x} \right| \Psi^{(0)}{}_k \right\rangle}{\mathrm{E}_k^{(0)} - \mathrm{E}_n^{(0)}} \text{, (13).}$$

The bracket terms in this relationship after substituting the wavefunction of the 1D-PIB given in Eqn. (10), evaluate as,

$$\left\langle \Psi^{(0)}{}_k \left| \hat{H}' \right| \Psi^{(0)}{}_n \right\rangle = \left\langle \Psi^{(0)}{}_n \left| \hat{H}' \right| \Psi^{(0)}{}_k \right\rangle = \frac{2}{L} \int_0^L x \cdot sin\left(\frac{n \pi x}{L} \right) \cdot sin\left(\frac{k \pi x}{L} \right) dx \text{ , (14),}$$

which after symbolical evaluation and simplification reduces to the following expression,

$$\left\langle \Psi^{(0)}{}_k \left| \hat{x} \right| \Psi^{(0)}{}_n \right\rangle = \frac{4 \cdot n \cdot k \cdot L\left[(-1)^{n+k} - 1 \right]}{\pi^2 \left(n^2 - k^2 \right)^2} \text{, (15).}$$

The 2nd order corrected energy of a wavefunction for the simple 1D-PIB is given by substitution of Eqns. (11) and (15) into Eqn. (13). This results to the following relationship,

$$\mathrm{E}_n^{(2)} = e^2 \cdot E^2 \sum_{n \neq k} \frac{\left(\frac{4 \cdot n \cdot k \cdot L\left[(-1)^{n+k} - 1 \right]}{\pi^2 \left(n^2 - k^2 \right)^2} \right)^2}{\frac{k^2 h^2}{8 m_e L^2} - \frac{n^2 h^2}{8 m_e L^2}} \text{, (16),}$$

that after a few algebraic steps reduces to,

$$\mathrm{E}_n^{(2)} = \frac{128 \cdot e^2 \cdot m_e \cdot L^4 \cdot E^2}{\pi^4 \cdot h^2} \sum_{n \neq k} \frac{n^2 \cdot k^2 \left[(-1)^{n+k} - 1 \right]^2}{\left(n^2 - k^2 \right)^5} \text{, (17).}$$

Using the 2nd order corrected energy of a wavefunction for the simple 1D-PIB one can calculate the polarizability tensor x-component using the definition of polarizability given in Eqn. (8). So the polarizability in the x-direction for the 1D-PIB is,

$$\alpha_{xx} = \frac{-256 \cdot e^2 \cdot m_e \cdot L^4}{\pi^4 \cdot h^2} \sum_{n \neq k} \frac{n^2 \cdot k^2 \left[(-1)^{n+k} - 1 \right]^2}{\left(n^2 - k^2 \right)^5}, \text{ (8),}$$

where m_e is the electron mass, L the length of the box, h Planck's constant, e the elementary charge of an electron and n and k the n^{th} and k^{th} energy levels, respectively.

Methodolgy in section C: Numerical polarizability for 1D-PIB with sinusoidal potential

Here we derive the equations required to numerically solve the 1D-PIB using the linear "shooting" method. Again the equation solved is the time-independent non-relativistic Schrödinger equation which for a single dimension is given by,

$$-\frac{\hbar^2}{2 m_e} \cdot \frac{\mathrm{d}^2 \Psi}{\mathrm{dx}^2} + \mathrm{V}\Psi = \mathrm{E}\Psi \text{ , (18)}$$

where $\hbar = h/2\pi$ and V is the potential under the influence of which electrons move. In the approach taken here, the potential is set equal to the sum of a sinusoidal potential generated by an array of nuclei and an isotropic homogeneous external electric field given by the expression,

$$\mathrm{V} = A \cdot \sin\left[2\pi (x + \varphi) \right] - q \cdot E \cdot x \text{ , (19),}$$

where A is the amplitude and φ is the phase of the sin-wave, respectively, and E the electric field strength. The external electric field is used to study the how the wavefunctions get polarized as a result of the perturbation by the field. Combining Eqns. (18) and (19) yield a second order differential equation that is solved numerically using the linear "shooting" method with the use of the boundary conditions that the wavefunctions have to vanish at x = 0 and x = L,

$$\frac{d^2\Psi}{dx^2}+\frac{2m_e}{\hbar^2}(E-A\cdot sin[2\pi(x+\varphi)]+q\cdot E\cdot x)\Psi=0\,,\ (20).$$

Once the eigenvalues, which satisfy the boundary conditions are found, the wavefunctions are evaluated which then can be used to calculate the polarizability,

$$\alpha=\frac{-\mu}{E}\,,\ (21),$$

where μ is the induced dipole moment given by the usual expression,

$$\mu=\frac{\int_0^L \Psi^*\,\hat{x}\,\Psi\,d\tau}{\int_0^L \Psi^*\Psi\,d\tau}\,,\ (22).$$

Our results show that the approximate treatment of 2nd order perturbation theory is sufficient to yield results as good as the exact numerical solutions. Differences between the two mathematical approaches are found to be less than 5%. We observe that as long as the perturbations studied are small, which is achieved by a small external electric field strength, the two methods yield comparable results.

References

1 F. London, Z. Physik **63**, 245 (1930).
2 C. D. Zeinalipour-Yazdi and D. P. Pullman, J. Phys. Chem. B **110**, 24260 (2006).
3 C. D. Zeinalipour-Yazdi, University of California, San Diego and San Diego State University, 2006.
4 D. C. Hanna, M. A. Yuratich, and D. Cotter, *Nonlinear optics of atoms and molecules*. (Springer, Berlin, 1979).
5 N. F. Lane, Rev. Mod. Phys. **52**, 29 (1980).
6 U. Hohm, J. Chem. Phys. **101**, 6362 (1994).
7 S. M. Lecours, H. W. Guan, S. G. Dimagno, C. H. Wang, and M. J. Therien, J. Am. Chem. Soc. **118**, 1497 (1996).
8 A. Vela and J. L. Gázquez, J. Am. Chem. Soc. **112**, 1490 (1990).
9 J. K. Nagle, J. Am. Chem. Soc. **112**, 4741 (1990).
10 B. Champagne and J.-M. André, Int. J. Quant.Chem. **42**, 1009 (1992).
11 V. Galiatsatos, R. O. Neaffer, S. Sen, and R. J. Sherman, *Physical properties of polymers handbook*. (AIP Press, Woodbury, 1996).
12 M. Zhou, Opt. Eng. **41**, 1631 (2002).
13 C. Jang and R. T. Chen, J. Lightware Technol. **21**, 1053 (2003).
14 S. Ahn and S. J. Shin, Sel. Top. Quantum Electron. **7**, 819 (2001).
15 C. Ma, H. Zhang, D. Zhang, Z. Cui, and S. Liu, Opt. Commun. **241**, 321 (2004).
16 P. Chopra, L. Carlacci, H. F. King, and P. N. Prasad, J. Phys. Chem. A **93**, 7120 (1989).
17 G. Maroulis and A. J. Thakkar, J. Chem. Phys. **95**, 9060 (1991).
18 E. F. Archibong and A. J. Thakkar, J. Chem. Phys. **98**, 8324 (1993).
19 H. S. Nalwa, J. Mukai, and A. Kakuta, J. Phys. Chem. A **99**, 10766 (1995).
20 D. Jacquemin, B. Champagne, and J. M. Andre, Int. J. Quantum Chem. **65**, 679 (1997).
21 B. Champagne, E. A. Perpète, S. J. A. van Gisbergen, E. J. Baerends, J. G. Snijders, C. S. Ghaoui, K. A. Robins, and B. Kirtman, J. Chem. Phys. **109**, 10489 (1998).
22 T. D. Poulsena, K. V. Mikkelsen, J. G. Fripiat, D. Jacquemin, and B. Champagne, J. Chem. Phys. **114**, 5917 (2001).
23 F. L. Gu, D. M. Bishop, and B. Kirtman, J. Chem. Phys. **115**, 10548 (2001).
24 B. Kirtman, B. Champagne, F. L. Gu, and D. M. Bishop, Int. J. Quantum Chem. **90**, 709 (2002).
25 A. Martinez, P. Otto, and J. Ladik, Int. J. Quantum Chem. **94**, 251 (2003).
26 (The tranverse polarizabilities in H_2^+ have a linear dependence ($L^{1.0}$) with respect to the internuclear hydrogen separation.).
27 K. N. Kudin and G. E. Scuseria, J. Chem. Phys. **113**, 7779 (2000).
28 J. M. Seminario, C. de la Cruz, P. A. Derosa, and L. Yan, J. Phys. Chem. B **108**, 17879 (2004).
29 J. August, H. W. Kroto, and N. Trinajstic, Astrophys. Space Sci. **128**, 411 (1986).
30 A. D. Slepkov, F. A. Hegmann, S. Eisler, E. Elliott, and R. R. Tykwinski, J. Chem. Phys. **120**, 6807 (2004).
31 S. Szafert and J. A. Gladysz, Chem. Rev. **103**, 4175 (2003).
32 D. Jacquemin, B. Champagne, and J.-M. André, Int. J. Quant.Chem. **65** (5), 679 (1997).
33 F. Sim, S. Chin, M. Dupuis, and J. E. Rice, J. Phys. Chem. **97**, 1158 (1993).

[34] E. K. Dalskov, J. Oddershede, and D. M. Bishop, J. Chem. Phys. **108** (5), 2152 (1998).
[35] J. A. Pople, J. W. McIver, and N. S. Ostlund, J. Chem. Phys. **49**, 2965 (1968).
[36] T. H. Jr. Dunning, J. Chem. Phys. **90**, 1007 (1989).
[37] H.-J. Werner, P. J. Knowles, R. Lindh, F. R. Manby, M. Schütz, P. Celani, T. Korona, G. Rauhut, R. D. Amos, A. Bernhardsson, A. Berning, D. L. Cooper, M. J. O. Deegan, A. J. Dobbyn, F. Eckert, C. Hampel, G. Hetzer, A. W. Lloyd, S. J. McNicholas, W. Meyer, M. E. Mura, A. Nicklass, P. Palmieri, R. Pitzer, U. Schumann, A. J. S. H. Stoll, R. Tarroni, and T. Thorsteinsson, MOLPRO 2006.1, a package of ab initio programs (2006).
[38] S. Grimme, J. Chem. Phys. **118**, 9095 (2003).
[39] W. H. Press, S. A. Teukolsky, W. T. Vetterling, and B. P. Flannery, *Numerical Recipes in C++*, 2nd ed. (Cambridge University Press, 2002).
[40] Maple 9.0 (Maplesoft, Waterloo, Ontario, 2003).
[41] G. P. Arrighini, N. Durante, C. Guidotti, and U. T. Lamanna, Theor. Chem. Acc. **104**, 327 (2000).
[42] M. Matsuura and T. Kamizato, Phys. Rev. B **33**, 8385 (1986).
[43] P. W. Atkins and R. S. Friedman, *Molecular Quantum Mechanics*, 3rd ed. (Oxford University Press, 1997).
[44] J. C. Jr. Morris, Phys. Rev. B **32**, 456 (1928).
[45] J. L. Toto, T. T. Toto, C. P. de Melo, B. Kirtman, and K. Robins, J. Chem. Phys. **104**, 8586 (1996).
[46] M. K. Shujiang Yang, J. Phys. Chem. A **110**, 9771 (2006).
[47] P. Botschwina, Chem. Phys. Lett. **47**, 241 (1982).
[48] E. Goldstein, B. Ma, J. H. Li, and N. L. Allinger, J. Phys. Org. Chem. **9**, 191 (1996).
[49] R. Peierls, *Quantum Theory of Solids*. (Clarendon, Oxford, 1955).
[50] A. Abdurahman, A. Shukla, and M. Dolg, Phys. Rev. B **65**, 115106 (2002).
[51] R. I. Keir, D. W. Lamb, G. L. D. Ritchie, and J. N. Watson, Chem. Phys. Lett. **279**, 22 (1997).